



1 **Performance of bias correction schemes for CMORPH**  
2 **rainfall estimates in the Zambezi River Basin**

3 **Webster Gumindoga<sup>1,2</sup>, Tom. H.M. Rientjes<sup>1</sup>, Alemseged.T. Haile<sup>3</sup>, Hodson Makurira<sup>2</sup> and Paolo**  
4 **Reggiani<sup>4</sup>**

5 <sup>1</sup>*Faculty ITC, University of Twente, The Netherlands*

6 <sup>2</sup>*Civil Engineering Department, University of Zimbabwe, Zimbabwe*

7 <sup>3</sup>*International Water Management Institute (IWMI), Ethiopia*

8 <sup>4</sup>*University of Siegen, Germany*

9

10 *Email of corresponding author: [w.gumindoga@utwente.nl](mailto:w.gumindoga@utwente.nl) OR [wgumindoga@gmail.com](mailto:wgumindoga@gmail.com)*  
11

---

12

13

14

15

16

17

18

19

20

21

22

23 *Email of corresponding author: [w.gumindoga@utwente.nl](mailto:w.gumindoga@utwente.nl)*  
24  
25  
26  
27  
28  
29  
30



31 **Abstract**

32 Satellite rainfall estimates (SRE) are prone to bias because such estimates are indirectly derived  
33 from visible, infrared, and/or microwave based information of cloud properties. We tested the  
34 influence of elevation and distance from large scale water bodies on bias for Climate Prediction  
35 Center-MORPHing (CMORPH) rainfall estimates. Effectiveness of five linear/non-linear and  
36 time-space variant/invariant bias correction schemes is evaluated. Evaluation also covers for  
37 different magnitudes of daily rainfall and climatic seasonality. We used daily rain gauge time  
38 series (1998-2013) from 60 stations, and counterparts from CMORPH time series for the  
39 Zambezi Basin. Taylor diagrams show that station elevation and distance from water bodies do  
40 not influence the estimation error of uncorrected CMORPH rainfall. For correction, the Spatio-  
41 temporal bias (STB) and Elevation zone bias (EZ) schemes showed best results in removing  
42 CMORPH rainfall bias for the Lower, Middle and Upper Zambezi subbasins. STB improved  
43 the correlation coefficient by 53 % and reduced the root mean squared difference by 25 %.  
44 Assessment of mean estimates by using a Taylor Diagram with mean estimates of correlation  
45 coefficient, root mean square difference and standard deviation showed that the EZ, Power  
46 transform, Distribution transformation and STB correction schemes best removed errors  
47 related to rainfall depth. Corrected CMORPH rainfall revealed an overestimation of very light  
48 rainfall (< 2.5 mm/day) and underestimation of very heavy rainfall (>20.0 mm/day) for all five  
49 correction schemes. Bias is best reduced for rainfall magnitudes of 0.0-2.5 and 5.0-10.0  
50 mm/day. Bias removal proved to be more effective in the wet season than in the dry season.

51

52 **Keywords:** *distance zone, elevation zone, satellite rainfall estimates, spatio-temporal bias,*  
53 *Taylor diagram*

54



55

56 **1. Introduction**

57

58 Correction schemes for rainfall estimates are developed for climate models (Maraun,  
59 2016;Grillakis et al., 2017;Switanek et al., 2017), for radar approaches (Cecinati et al.,  
60 2017;Yoo et al., 2014) and for satellite based, multi-sensor, approaches (Najmaddin et al.,  
61 2017;Valdés-Pineda et al., 2016). In this study focus is on satellite rainfall estimates (SRES)  
62 so to improve reliability in water resource applications.

63

64 Studies in satellite based rainfall estimation show that estimates are prone to systematic and  
65 random errors (Gebregiorgis et al., 2012;Habib et al., 2014;Shrestha, 2011;Tefsagiorgis et al.,  
66 2011;Vernimmen et al., 2012;Woody et al., 2014). Errors result primarily from the indirect  
67 estimation of rainfall from visible (VIS), infrared (IR), and/or microwave (MW) based satellite  
68 remote sensing of cloud properties (Pereira Filho et al., 2010;Romano et al., 2017). Systematic  
69 errors in SREs commonly are referred to as bias, which is a measure that indicates the  
70 accumulated difference between rain gauge observations and SREs. Bias in SREs is expressed  
71 for rainfall depth and volume (Habib et al., 2012b), rain rate (Haile et al., 2013) and frequency  
72 at which rain rates occur (Khan et al., 2014). Bias may be negative or positive where negative  
73 bias indicates underestimation whereas positive bias indicates overestimation (Liu,  
74 2015;Moazami et al., 2013).

75

76 Studies (Wehbe et al., 2017;Jiang et al., 2016;Liu et al., 2015;Haile et al., 2015) reveal that  
77 CMORPH satellite rainfall has variable accuracy across different regions. As such correction  
78 schemes serve to correct for systematic errors and to improve applicability of SREs. Correction  
79 schemes rely on assumptions that adjust errors in space and/or time (Habib et al., 2014). Some  
80 correction schemes consider correction only for spatial distributed patterns in bias, commonly  
81 known in literature as space variant/invariant. Approaches that correct for spatially averaged  
82 bias have roots in radar rainfall estimation (Seo et al., 1999) but are unsuitable for large scale  
83 basins (> 5,000 km<sup>2</sup>) where rainfall may substantially vary in space (see Habib et al., 2014).  
84 Studies by Tefsagiorgis et al. (2011) in Oklahoma (USA) and Müller and Thompson (2013) in  
85 Nepal concluded that space variant correction schemes are more effective in reducing  
86 CMORPH and TRMM bias than space invariant correction schemes. In Bhatti et al. (2016), for  
87 the Upper Blue Nile basin in Ethiopia, it is shown that CMORPH bias correction is most  
88 effective when bias correction is for periods of 6 days.

89

90 Bias correction schemes based on regression techniques have reported distortion of frequency  
91 of rainfall rates (Ines and Hansen, 2006;Marcos et al., 2018). Multiplicative shift procedures  
92 tend to adjust SRE rainfall rates, but Ines and Hansen (2006) reported that they do not correct  
93 systematic errors in rainfall frequency of climate models. Non-multiplicative bias correction  
94 schemes preserve the timing of rainfall within a season (Fang et al., 2015;Hempel et al., 2013).



95 **Studies** that have applied non-linear bias correction schemes such as Power function report  
96 correction of extreme values (depth, rate and frequency) thus mitigating the underestimation  
97 and overestimation of CMORPH rainfall (Vernimmen et al., 2012). The study by Tian (2010)  
98 in the United States noted that the Bayesian (likelihood) analysis techniques are found to over-  
99 adjust both light and heavy satellite rainfall toward moderate CMORPH rainfall.

100

101 Bias often exhibits a topographic and latitudinal dependency as, for instance, shown for the  
102 National Oceanic and Atmospheric Administration (NOAA) **Climate Prediction Center-**  
103 **MORPHing** (CMORPH) product in the Nile Basin (Bitew et al., 2011; Habib et al., 2012a; Haile  
104 et al., 2013). For Southern Africa, Thorne et al. (2001), Dinku et al. (2008) and Meyer et al.  
105 (2017) show that bias in rainfall rate and frequency can be related to location, topography, local  
106 climate and season. First studies in the Zambezi Basin (Southern Africa) on SREs show  
107 evidence that necessitates correction of SREs. For example Cohen Liechti (2012) show bias in  
108 CMORPH SREs for daily rainfall and for accumulated rainfall at monthly scale. Matos et al.  
109 (2013), Thiemiig et al. (2012) and Toté et al. (2015) show that bias in rainfall depth at time  
110 steps ranging from daily to monthly varies across geographical domains in the Zambezi Basin  
111 and may be as large as  $\pm 50\%$ . Besides topographic effects, rainfall is affected by presence of  
112 large scale water bodies which influences surface or atmospheric properties (Haile et al.,  
113 2009; Rientjes et al., 2013). As such, SREs may be affected as well ~~necessitating to correct for~~  
114 ~~bias by~~ presence of large scale water bodies.

115

116 For ~~less developed~~ areas such as ~~in the~~ Zambezi Basin ~~that is~~ selected for this study,  
117 applications of SREs are ~~very~~ limited. **This is despite the strategic importance of the basin in**  
118 **providing water to over 50 million people.** An exception is the study by Beyer et al. (2014) on  
119 correction of the TRMM-3B42 product for agricultural purposes in the Upper Zambezi Basin.  
120 First studies on use of SREs in the Zambezi River Basin mainly focused on accuracy  
121 assessment of the SREs using standard statistical indicators with little or no effort to perform  
122 bias correction despite the evidence of errors in these products. The use of uncorrected satellite  
123 rainfall is reported for hydrological modelling in the Nile Basin (Bitew and Gebremichael,  
124 2011) and Zambezi Basin (Cohen Liechti et al., 2012), respectively, and for drought monitoring  
125 in Mozambique (Toté et al., 2015). The above studies highlight the demand for the use of  
126 corrected SREs for improved water resources management. Our selection of CMORPH  
127 satellite rainfall for this study is based on successful applications of bias corrected CMORPH  
128 estimates in African basins for hydrological modelling (Habib et al., 2014) and flood  
129 predictions in West Africa (Thiemiig et al., 2013). In first publications on CMORPH, Joyce et  
130 al. (2004) describe CMORPH as a gridded precipitation product that estimates rainfall with  
131 information derived from IR data and MW data. CMORPH combines the retrieval accuracy of  
132 passive MW estimates with IR measurements which are available at high temporal resolution  
133 but with lower accuracy. The important distinction between CMORPH and other merging  
134 methods is that the IR data are not used for rainfall estimation but ~~used~~ only to propagate



135 rainfall features that have been derived from microwave data. The flexible ‘morphing’  
136 technique is applied to modify the shape and rate of rainfall patterns. CMORPH is operational  
137 since 2002 for which data is available at the CPC of the National Centers for Environmental  
138 Prediction (NCEP) (after <http://www.ncep.noaa.gov/>). Recent publications on CMORPH exist  
139 (Wehbe et al., 2017; Koutsouris et al., 2016; Jiang et al., 2016; Haile et al., 2015).

140

141 In this study we use CMORPH and rain gauge data for Upper, Middle, and Lower Zambezi  
142 basins to (1) test whether the performance of CMORPH rainfall estimates is affected by  
143 elevation and distance from large water bodies, (2) evaluate the effectiveness of linear/non-  
144 linear and time-space variant/invariant bias correction schemes and (3) assess the performance  
145 of bias correction schemes to represent different rainfall magnitudes for climate seasonality.  
146 The above improves reliability in water resource applications in the Zambezi basin such as in  
147 drought analysis, flood prediction, weather forecasting and rainfall-runoff modeling.

148

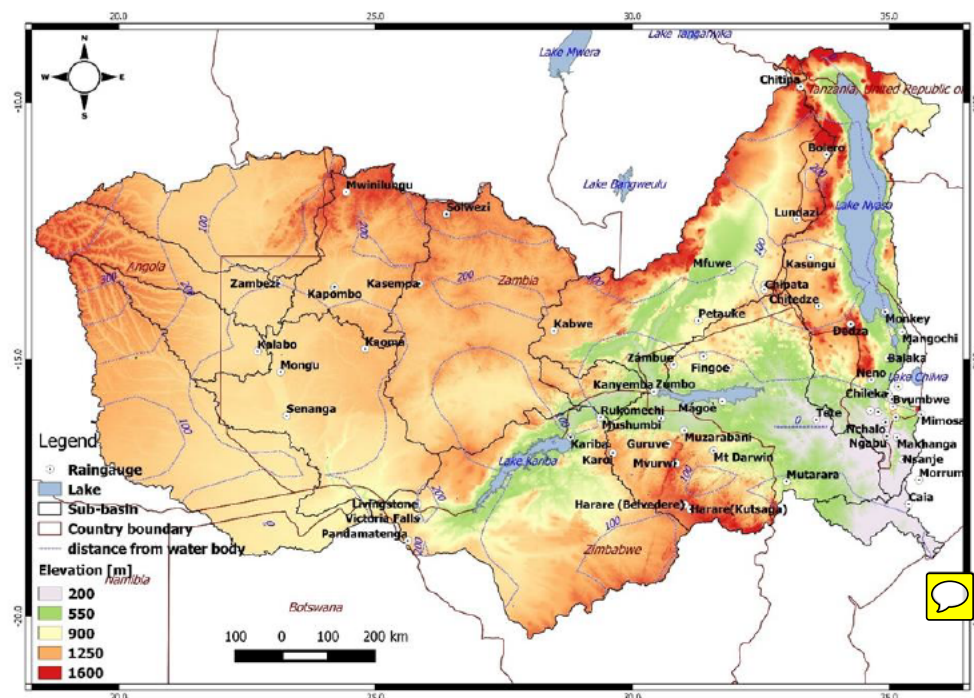
## 149 2. Study area

150 The Zambezi River is the fourth-longest river (~2,574 km) in Africa with basin area of  
151 ~1,390,000 km<sup>2</sup> (~4 % of the African continent). The river drains into the Indian Ocean and  
152 has mean annual discharge of 4,134 m<sup>3</sup>/s (World Bank, 2010b). The river has its source in  
153 Zambia and forms boundaries of Angola, Namibia, Botswana, Zambia, Zimbabwe and  
154 Mozambique (Fig. 1). The basin has considerable differences in elevation, topography and  
155 climatic seasons and, as such, makes the basin well suited for this study. The basin is divided  
156 into three subbasins i.e., the Lower Zambezi comprising the Tete, Lake Malawi/Shire, and  
157 Zambezi Delta basins, the Middle Zambezi made up of the Kariba, Mupata, Kafue, and  
158 Luangwa basins, and the Upper Zambezi constituted by the Kabompo, Lungwebungo,  
159 Luanginga, Barotse, and Cuando/Chobe basins (Beilfuss, 2012).

160

161 The elevation of the Zambezi basin ranges from < 200 m (for some parts of Mozambique) to  
162 >1500 m above sea level (for some parts of Zambia). Large scale water bodies in and around  
163 the basin are Kariba, Cabora Bassa, Bangweulu, Chilwa and Nyasa. The Indian Ocean is to the  
164 east of Mozambique. Typical landcover types are woodland, grassland, water surfaces and  
165 cropland (Beilfuss et al., 2000). The basin is characterized by high annual rainfall (>1,400  
166 mm/yr) in the northern and north-eastern areas but low annual rainfall (<500 mm/yr) in the  
167 southern and western parts (World Bank, 2010a). Due to this rainfall distribution, northern  
168 tributaries in the Upper Zambezi subbasin contribute 60-% of the mean annual discharge  
169 (Tumbare, 2000). The river and its tributaries are subject to seasonal floods and droughts that  
170 have devastating effects on the people and economies of the region, especially the poorest  
171 members of the population (Tumbare, 2005). It is not uncommon to experience both floods and  
172 droughts within the same hydrological year.

173



174 Figure 1: Zambezi River Basin with sub basins, major lakes, rivers, elevation and locations of the 60 rain gauging stations  
175 used in this study The Euclidian distance (km) from large scale water bodies is also shown

176

### 177 3. Materials and Methodology

178

#### 179 3.1. Data

180

##### 181 3.1.1. CMORPH rainfall

182 For this study time series (1998-2013) of CMORPH rainfall product at  $8 \text{ km} \times 8 \text{ km}$ , 30-minute  
183 resolution are selected. Images were downloaded from the GeoNETCAST ISOD toolbox by  
184 means of ILWIS GIS software (<http://52north.org/downloads/>). We aggregated half hourly data  
185 to daily totals to match the gauge based counter-parts.

186

##### 187 3.1.2. Rain gauge rainfall

188 Time series of daily rainfall from 66 stations was obtained from meteorological departments in  
189 Botswana, Malawi, Mozambique, Zambia and Zimbabwe that cover the study area. After  
190 screening, 6 stations with unreliable time series were removed. Although a number of the 60  
191 remaining stations are affected by data gaps, the available time series are of sufficiently long  
192 duration to serve the objectives of this study. The location of the stations cover elevation values  
193 that range from 3 m to 1600 m asl. and distance to a large scale water bodies that range from  $\leq$   
194 10 km to  $\geq$  500 km. This allows us to assess the effect of the above factors on SRE performance.

195



### 196 3.2. Topographic influences: Elevation and distance from lake water bodies

197 Studies such as in the Nile Basin (Habib et al., 2012a; Haile et al., 2009; Rientjes et al., 2013)  
198 reveal that elevation and distance from lake water bodies interact to produce unique circulation  
199 patterns that affect the performance of SREs. This study investigated topographic influences  
200 on rainfall distribution, frequency and rain rate by analysing effects of elevation and distance  
201 of the 60 rain gauges to large scale water bodies in the Zambezi Basin (See Table 1). As such  
202 the hierarchical cluster ‘within-groups linkage’ method in the Statistical Product and Service  
203 Solutions (SPSS) software was used to classify the Zambezi Basin into 3 elevation zones. These  
204 are zone 1: elevation of < 250 m (mean elevation  $\approx$  90 m), zone 2: elevation range of 250- 950  
205 m (mean elevation  $\approx$  510 m) and zone 3: elevation > 950 m (mean elevation  $\approx$  1140 m). Based  
206 on rain gauge Euclidian distance to large scale water bodies 4 arbitrary distance zones are  
207 defined. These are zone 1: < 10 km (mean distance = 5 km), zone 2: 10 - 50 km (mean distance  
208 = 35 km), zone 3: 50 -100 km (mean distance = 80 km) and zone 4: > 100 km (mean distance  
209 = 275 km). The Advanced Spaceborne Thermal Emission and Reflection Radiometer (ASTER)  
210 based DEM of 30 m resolution obtained from <http://gdem.ersdac.jspacesystems.or.jp/>, was  
211 used for representing elevation across the Zambezi Basin. The Euclidian distance of each rain  
212 gauge location to large scale water bodies was computed in a GIS environment through the  
213 distance calculation algorithm. Large scale water bodies are defined as perennial water bodies  
214 with surface area  $\geq$  700 km<sup>2</sup>.

215

### 216 3.3. Bias correction schemes

217 In this study, the bias in CMORPH rainfall estimates was assessed and corrected using five  
218 schemes. We note that findings on performance of bias correction schemes in literature do not  
219 allow generalization but only apply to the respective study domains. Based on the above studies  
220 we selected five approaches for evaluation for the Zambezi Basin. These are the Spatio-  
221 temporal bias (STB), Elevation zone bias (EZB), Power transform (PT), Distribution  
222 transformation (DT), and the Quantile mapping based on an empirical distribution (QME). The  
223 five schemes are chosen based on merits documented in literature and the aim of the present  
224 work to adjust for CMORPH rainfall variability in space and/or time. Following Habib et al.  
225 (2014) and Bhatti et al. (2016), and based on preliminary analysis in this study on rainfall  
226 distributions in the Zambezi Basin, the bias correction factor is calculated for a certain day only  
227 when a minimum of five rainy days were recorded within the preceding 7-day window with a  
228 minimum rainfall accumulation depth of 5 mm, otherwise no bias is estimated (i.e. a value of 1  
229 applies as bias correction factor). This approach implies that bias factors change value for each  
230 station for each 7-day period.

231

232 In the approach, a time window of specified length moves forward in the time domain. Bhatti  
233 et al. (2016) in the Lake Tana basin (Ethiopia) carried out a sensitivity analysis on moving  
234 windows where bias factor change for each day, and on sequential windows were bias factor  
235 is constant for the window length. Tests for window lengths of 3, 5, 7, ..., 31 days indicated



236 that a 7-day sequential time window is most appropriate for bias correction. Also in the present  
 237 a 7-day moving time window is adopted by preliminary analysis with accumulated rainfall of  
 238 minimum 5 mm that occurred over at least 5 rainy days during the 7-day window. Preliminary  
 239 analysis of wet season rainfall on all gauges in the Zambezi Basin indicates that the criterion  
 240 in Bhatti et al. (2016) are commonly met so the above thresholds are adopted for this study.

241

### 242 3.3.1. Spatio-temporal bias correction (STB)

243 This linear bias correction scheme has its origin in the correction of radar based precipitation  
 244 estimates (Tsefagiorgis et al., 2011) and downscaled precipitation products from climate  
 245 models. The CMORPH daily rainfall estimates ( $S$ ) are multiplied by the bias correction factor  
 246 for the respective moving time windows for individual stations resulting in corrected  
 247 CMORPH estimates ( $S_{STB}$ ) in a temporally and spatially coherent manner (Equation [1]).

248

$$249 \quad S_{STB} = S \frac{\sum_{t=d}^{t=d-l} S(i,t)}{\sum_{t=d}^{t=d-l} G(i,t)} \quad [1]$$

250 Where:

251  $G$  = daily gauge based rainfall observations252  $i$  = gauge location253  $d$  = selected day254  $t$  = julian day number255  $l$  = length of a time window for bias calculation

256

257 The advantages of the bias scheme are the simplicity and modest data requirements and that it  
 258 adjusts the daily mean of CMORPH at each station.

259

### 260 3.3.2. Elevation zone bias correction (EZ).

261 This bias scheme is proposed in this study and aims at correction of satellite rainfall as affected  
 262 by topographic and landsurface influences. The method groups rain gauge stations into 3  
 263 elevation zones (see section 3.2) based on station elevation. The grouping in this study is based  
 264 on the hierarchical clustering technique as also guided by knowledge of the study area. The  
 265 assumption is that a number of stations ( $n$ ) in the same elevation zone have the same bias  
 266 characteristics and are assigned a spatially invariant but temporally variant bias correction  
 267 factor with a different bias factor for each 7-day window. The corrected CMORPH estimates  
 268 ( $S_{EZ}$ ) at daily base are obtained by multiplying the uncorrected the CMORPH daily rainfall  
 269 estimates ( $S$ ) by the daily bias factor in each elevation zone.

270

$$271 \quad S_{EZ} = S \frac{\sum_{t=d}^{t=d-l} \sum_{i=1}^{i=n} S(i,t)}{\sum_{t=d}^{t=d-l} \sum_{i=1}^{i=n} G(i,t)} \quad [2]$$

272





273 The merits of this bias correction scheme is that the daily time variability is preserved but also  
274 effects of elevation is accounted for.

275

### 276 3.3.3. Power transform (PT)

277 In Lafon et al. (2013) it is described that the nonlinear *PT* bias correction scheme has its origin  
278 in general circulation models. Vernimmen et al. (2012) revealed an application to correct  
279 satellite rainfall estimates for hydrological modelling and drought monitoring. The daily bias  
280 corrected CMORPH rainfall (*SPT*) is obtained using:

281

$$282 \quad SPT = aG(i,t)^b \quad [3]$$

283 Where

284  $G$  = daily rain gauge rainfall

285  $a$  = prefactor such that the mean of the transformed CMORPH values is equal to the  
286 mean of gauge observations

287  $b$  = factor calculated such that for each station the coefficient of variation (CV) of  
288 CMORPH matches the gauge based observation

289  $i$  = gauge location

290  $t$  = julian day number

291

292 Optimized values for  $a$  and  $b$  are obtained through the generalized reduced gradient algorithm  
293 (Fylstra et al., 1998). Values for  $a$  and  $b$  vary within the 7-day time window since correction is  
294 at daily time base. The advantage of the *PT* scheme is that rainfall variability of the daily time  
295 series is preserved by adjusting both the mean and standard deviation of the CMORPH  
296 estimates. The bias scheme also adjusts extreme precipitation values in CMORPH estimates  
297 (Vernimmen et al., 2012).

298

### 299 3.3.4. Distribution transformation (DT)

300 This additive approach to bias correction has its origin in statistical downscaling of climate  
301 model data (Bouwer et al., 2004). In this study, the method determines the statistical  
302 distribution function at daily base of all rain gauge station observation as well as CMORPH  
303 values at the respective stations. The CMORPH statistical distribution function is matched from  
304 the rain gauge data distribution following the steps described in equations [4-8]. Both the  
305 difference in mean value and the difference in variation are corrected. First the bias correction  
306 factor for the mean *DTu* is determined following Equation [4]:

307

$$308 \quad DTu = \frac{Gu}{Su} \quad [4]$$

309  $Gu$  and  $Su$  are mean values of 7-day gauge and CMORPH rainfall estimates for gauged  
310 counterparts.

311



312 Secondly, the correction factor for the variation ( $DT\tau$ ) is determined by the quotient of the 7-  
313 day standard deviations,  $G\tau$  and  $S\tau$ , for gauge and CMORPH respectively.

314

$$315 \quad DT\tau = \frac{G\tau}{S\tau} \quad [5]$$

316 Once the correction factors are established, varying within a 7-day time window, factors are  
317 applied to correct all daily CMORPH estimates ( $S$ ) through equation [6] to obtain corrected  
318 CMORPH rainfall estimate ( $S_{DT}$ ).

319

$$320 \quad S_{DT} = (S(i, t) - S_u)DT\tau + DTu * S\tau \quad [6]$$

321 To ensure non-negative values, the formula was modified to result in the retention of the  
322 uncorrected CMORPH daily values. The merit of this bias scheme is that it corrects for  
323 frequency-based indices such as standard deviation and percentile values (Fang et al., 2015).

324

### 325 3.3.5. Quantile mapping based on an empirical distribution (QME)

326 This is a quantile based empirical-statistical error correction method with its origin in empirical  
327 transformation and bias correction of regional climate model-simulated precipitation (Thiemeßl  
328 et al., 2012). The method corrects CMORPH precipitation ( $S$ ) based on point-wise constructed  
329 empirical cumulative distribution functions (*ecdfs*) on a 7-day time window. Rainfall frequency  
330 is corrected at the same time (Thiemeßl et al., 2010).

331

332 The bias corrected rainfall ( $S_{QME}$ ) using quantile mapping can be expressed in terms of the  
333 empirical cumulative distribution function (*ecdf*) and its inverse ( $ecdf^{-1}$ ) that are developed on  
334 a 7-day time window but with new values for each day.

335

$$336 \quad S_{QME} = ecdf_{obs}^{-1}(ecdf_{raw}(S(i, t))) \quad [7]$$

337

338 Where:

339  $ecdf_{obs}$  = empirical cumulative distribution function for the gauge based observation

340  $ecdf_{raw}$  = empirical cumulative distribution function for the uncorrected CMORPH

341

342 The advantage of this bias scheme is that it corrects bias in the mean, standard deviation (Fang  
343 et al., 2015) as well as errors in rainfall depth. The approach is important for long term water  
344 resources assessments under the influence of land use or climate change. Furthermore, it  
345 preserves the extreme precipitation values (Thiemeßl et al., 2012).

346

### 347 3.4. Evaluation according to rainfall magnitudes and seasons

348 Performance of SREs for different rainfall rate classes and for different seasons is distinct  
349 across the Zambezi river basin. As such five classes are defined that are 0.0-2.5, 2.5-5.0, 5.0-  
350 10.0, 10.0-20.0 and >20.0 mm/day to explore accuracy of CMORPH on different classification



351 of magnitude of daily rainfall. Classes indicate very light (< 2.5 mm/day), light (2.5-5.0),  
352 moderate (5.0-10.0 mm/day), heavy (10.0-20.0 mm/day) and very heavy rainfall (> 20  
353 mm/day) respectively.

354

355 Furthermore, CMORPH rainfall time series were divided into wet and dry seasonal periods to  
356 assess the influence of seasonality on performance of bias correction schemes. The wet season  
357 in Southern Africa spans from October-March whereas the dry season spans from April-  
358 September.

359

### 360 3.5. Performance evaluation of bias corrected rainfall

361 A comparison of corrected and uncorrected CMORPH satellite rainfall estimates with rain  
362 gauge data was performed using statistics that measure systematic differences (i.e. percentage  
363 bias), measures of association (e.g. correlation coefficient) and random differences (e.g.  
364 standard deviation of differences and coefficient of variation) (Haile et al., 2013). Bias is a  
365 measure of how the satellite rainfall estimate deviate from the raingauge estimate, and the result  
366 is normalised by the summation of the gauge values. The correlation coefficient (ranging  
367 between +1 and -1) represents the linear **interdependence** of gauge and CMORPH data.

368

369 Equations [8-9] apply.

370

$$371 \text{ bias (\%)} = \frac{\sum(S-G)}{\sum G} * 100 \quad [8]$$

372

$$373 R = \frac{\sum(G-\bar{G})(S-\bar{S})}{\sqrt{\sum(G-\bar{G})^2} \sqrt{\sum(S-\bar{S})^2}} \quad [9]$$

374

375 Where:

376  $S$  = rainfall estimates by a satellite (mm/day)

377  $\bar{S}$  = mean values of the satellite rainfall estimates (mm/day)

378  $G$  = rainfall recorded by a rain gauge (mm/day)

379  $\bar{G}$  = mean values of rainfall recorded by a rain gauge (mm/day)

380

### 381 3.6. Assessment through Taylor diagram

382 Visual comparison of performance of SREs was done using Taylor diagrams which provide a  
383 statistical summary of how well patterns match each other in terms of the Pearson's product-  
384 moment correlation coefficient ( $R$ ), root mean square difference ( $E$ ), and the **ratio of variances**  
385 on a 2-D plot (Lo Conti et al., 2014; Taylor, 2001). The reason that each point in the two-  
386 dimensional space of the Taylor diagram can represent the above three different statistics  
387 simultaneously is that the centered pattern of root mean square difference ( $E^i$ ), and the ratio of  
388 variances are related by the following:

389



$$E^i = \sqrt{\sigma_f^2 + \sigma_r^2 - 2\sigma_f\sigma_r R} \quad [10]$$

391

392 Where:

393  $\sigma_f$  and  $\sigma_r$  = standard deviation of CMORPH and rain gauge rainfall, respectively.

394

395 Applications of Taylor diagrams have roots in climate change studies (Smiatek et al.,  
396 2016; Taylor, 2001) but also has frequent applications in environmental model evaluation  
397 studies (Cuvelier et al., 2007; Dennis et al., 2010; Srivastava et al., 2015). Bhatti et al., (2016)  
398 propose the use of Taylor Diagrams for assessing effectiveness of SREs bias correction  
399 schemes. The merits of the five bias correction schemes used in this study can be inferred from  
400 the Taylor diagram. The most effective bias correction schemes will have data that lie near a  
401 point marked 'reference' on the x-axis, relatively high correlation coefficient and low root  
402 mean square difference. Bias corrections schemes matching gauged-based standard deviation  
403 have patterns that have the right amplitude.

404

#### 405 4. Results and Discussion

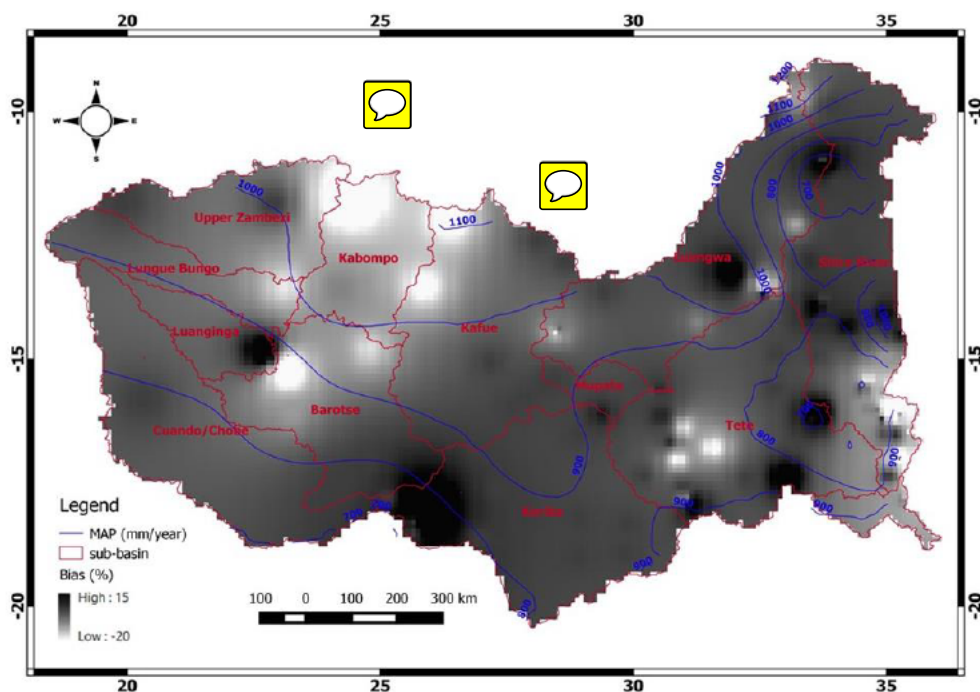
406

##### 407 4.1. Performance of uncorrected CMORPH rainfall

408

409 The spatially interpolated values of bias (%) covering the Zambezi Basin are shown in Figure  
410 2. Areas in the central and western part of the basin have bias relatively close to zero suggesting  
411 good performance of the uncorrected CMORPH product. However large negative bias values  
412 are shown in the south-eastern part of the basin such as Shire River Basin, and in the Upper  
413 Zambezi's high elevated areas such as Kabompo and northern Barotse Basin. Significant  
414 underestimation is found in the Lower Zambezi's downstream areas where the Zambezi River  
415 enters the Indian Ocean. Generally, CMORPH overestimates rainfall locally in Kariba,  
416 Luanginga, and Luangwa basins. As such CMORPH estimates do not consistently provide  
417 results that match gauge observations. We note that the rain gauge network with poor density  
418 could have attributed to the findings on bias by poor rainfall representation of spatially  
419 interpolated rainfall. Since CMORPH estimates have large error ( $10 < \text{bias} (\%) < -10$ ), we first  
420 need to remove the bias before the product may be applied in hydrological and water resources  
421 applications. Figure 2 also show contours for rain gauge mean annual precipitation (MAP) in  
422 the Zambezi Basin with higher values in the northern parts of the basin (Kabompo and  
423 Luangwa) compared to the of lower localised estimates of MAP such as in Shire River and  
424 Kariba subbasins.

425



426 Figure 2: The spatial variation of bias (%) estimate for gauge vs CMORPH daily rainfall (1998-2013) for the Zambezi Basin  
427 The CMORPH Mean Annual Precipitation (MAP) is also shown as blue contours

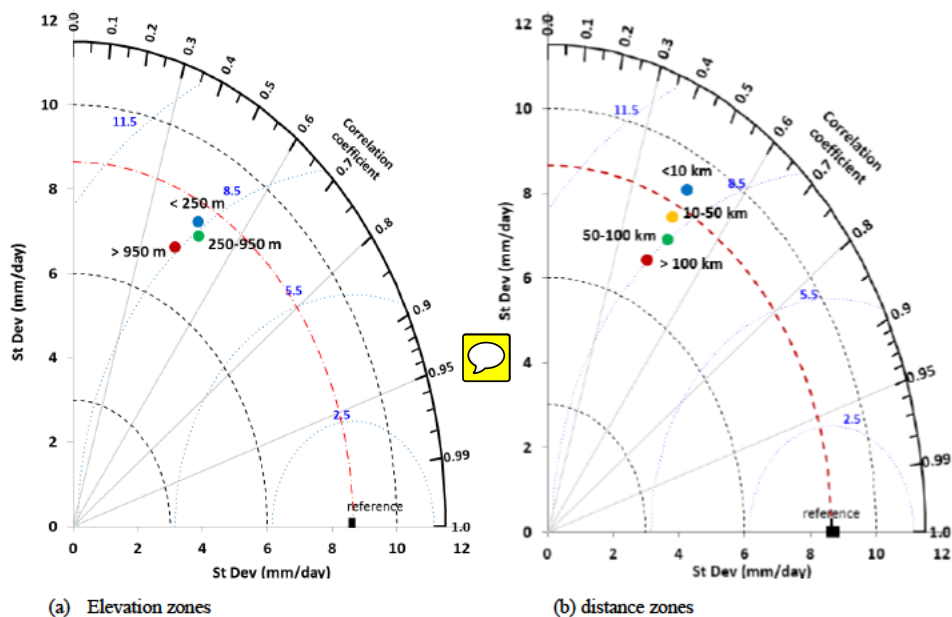
428

#### 429 4.2. Topographic influences for CMORPH and gauge rainfall

430 Figure 3 shows Taylor diagrams with a comparison of basin lumped estimates of daily  
431 uncorrected time series (1998–2013) of CMORPH and rain gauge observations for the 3  
432 elevation zones (left panes) and 4 distance zones from large scale water bodies (right panes).  
433 The purpose of the diagrams is to show dependency of CMORPH and gauge rainfall on  
434 elevation or distance from large scale water bodies. Findings indicate that both elevation and  
435 distance from a large water body have no influence on the CMORPH error estimates because  
436 the standard deviations in the elevation zones and the distance zones from large scale water  
437 bodies (except for the < 10 km distance zone) are lower than the reference/rain gauge standard  
438 deviation which is indicated by the dashed brown arc (value of 8.45 mm/day). Figure 3 reveals  
439 that the standard deviations in the elevation zones and the distance zones (except for the < 10  
440 km distance zone) are lower than the reference/rain gauge standard deviation which is indicated  
441 by the dashed brown arc (value of 8.45 mm/day). The stations in the high elevation zone (>  
442 950 m) and long distance zone (> 100 km) reveal lower variability than stations at lower  
443 elevation and shorter distance zones. With respect to the reference line, CMORPH estimates  
444 lumped for respective elevation zones and distance to a large water body do not match standard  
445 deviation of rain gauge based counterparts. Also, a low correlation coefficient ( $R$ ) is shown with  
446 high root mean square difference ( $E$ ) as compared to gauge based estimates (Figure 3). Overall,  
447 statistics (standard deviations,  $R$  and root mean square error) for uncorrected CMORPH show



448 poor performance compared to the gauge based estimates but also do not vary for increasing  
 449 or decreasing elevation and distance from large scale water bodies. This is despite that the  
 450 intermediate elevation zone (250-950 m) and the intermediate distance zone (50-100 km) show  
 451 a slightly better match to CMORPH estimates.  
 452



453 (a) Elevation zones (b) distance zones  
 454 Figure 3 Time series of rain gauge (reference) vs CMORPH estimations, period 1998-2013, for elevation zones (left panes)  
 455 and distance zones (right panes) in the Zambezi Basin. The correlation coefficients for the radial line denote the relationship  
 456 between CMORPH and gauge based observations. Standard deviations on both the x and y axes show the amount of variance  
 457 between the two time series. The standard deviation of the CMORPH pattern is proportional to the radial distance from the  
 458 origin. The angle between symbol and abscissa measures the correlation between CMORPH and rain gauge observations. The  
 459 root mean square difference (blue contours) between the CMORPH and rain gauge patterns is proportional to the distance to  
 460 the point on the x-axis identified as "reference". For details, see Taylor (2001)

461  
 462 Results indicate that aspects of elevation and distance from large water bodies are not  
 463 distinctively represented (no clear signature) in the relationship between CMORPH and gauge  
 464 rainfall in the Zambezi Basin. For elevation, Vernimmen et al. (2012) had a similar conclusion  
 465 in Indonesia (Jakarta, Bogor, Bandung, Java, Kalimantan and Sumatra regions) since a  
 466 relationship for TRMM Multi-satellite Precipitation Analysis (TMPA) 3B42RT precipitation  
 467 against elevation could not be identified ( $R^2 = 0.0001$ ). The study by Gao and Liu (2013)  
 468 showed that the bias in CMORPH rainfall over the Tibetan Plateau present weak dependence  
 469 on elevation. Contrary to these findings, Romilly and Gebremichael (2011) showed that the  
 470 accuracy of CMORPH at monthly time base is related to elevation for six river basins in  
 471 Ethiopia. Whilst distance from large lake water bodies and elevation have been assessed  
 472 separately for this study, Habib et al. (2012a) revealed that the two interact in the Nile Basin to  
 473 produce unique circulation patterns to affect the performance of SRE.  
 474



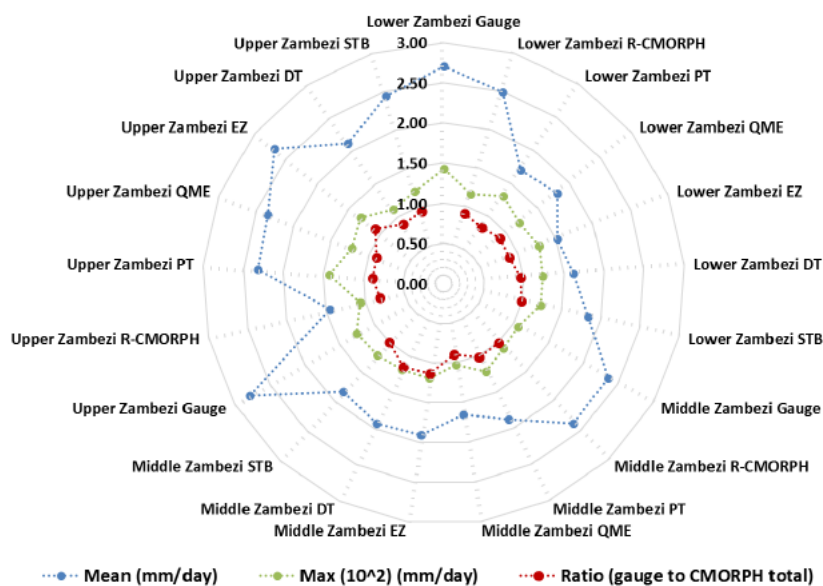
475 **4.3. Rainfall bias correction**

476

477 **4.3.1. Assessment of CMORPH bias correction effectiveness**

478 The statistics for the gauge, uncorrected and bias corrected satellite rainfall for the Lower,  
 479 Middle and Upper Zambezi subbasins are shown in Figure 4. Using the standard statistics  
 480 (mean, maximum and ratio of gauge totals to CMORPH totals), the bias of CMORPH estimates  
 481 has been moderately reduced by applying the five bias correction schemes. However, the  
 482 effectiveness of the schemes vary spatially with best performance in Lower and Upper Zambezi  
 483 subbasin and relatively poor performance in the Middle Zambezi subbasin (see Figure 4).

484



485

486 Figure 4: Frequency based statistics (mean, max, ratio of gauged sum vs CMORPH sum for 1998-2013) for the Zambezi Basin  
 487

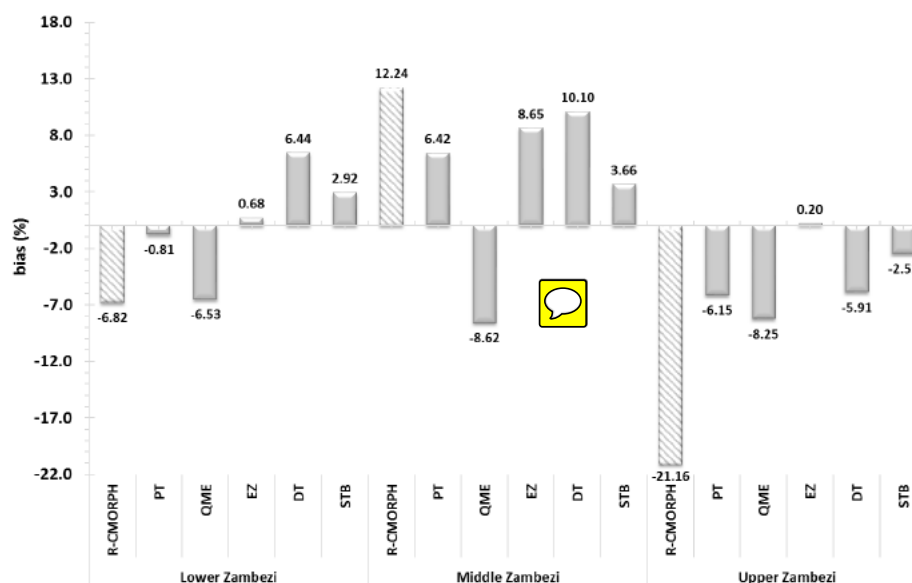
488 Results indicate that STB bias correction scheme is consistently effective in removing  
 489 CMORPH rainfall bias in the Zambezi Basin judging by all performance indicators. However,  
 490 we observe that performance of the bias schemes depend on the objective they are originally  
 491 designed for, such as, for instance, that STB and PT adjust for the mean of CMORPH rainfall  
 492 estimates. Statistics in Figure 5 confirm these findings especially for the Upper Zambezi  
 493 subbasin where the mean of corrected CMORPH estimates improved by > 60% from the mean  
 494 of uncorrected estimates. In addition, PT in the Lower Zambezi, QME in both Middle and  
 495 Upper Zambezi and STB in the Upper Zambezi were also effective (improvement by 16 %) in  
 496 correcting for the highest values in the rainfall estimates. The STB performs better than other  
 497 bias schemes in reproducing rainfall for the Lower and Upper Zambezi subbasin, where the  
 498 ratio of gauge total to corrected CMORPH total is 1.0.

499



500 Figure 5 shows the percentage bias in corrected and uncorrected CMORPH daily rainfall  
 501 (1998-2013) averaged for the Lower, Middle and Upper Zambezi basins. The effectiveness of  
 502 the bias correction by all schemes varies over the different parts of the basin but is higher in  
 503 Lower and Upper than in Middle Zambezi.

504



505

506 Figure 5: Percentage bias of corrected and uncorrected CMORPH daily rainfall averaged for the Lower Zambezi, Middle  
 507 Zambezi and Upper Zambezi. Brown bars=uncorrected CMORPH and blue = bias corrected CMORPH

508

509 With regard to reducing bias, best results are obtained by EZ in the Lower Zambezi (percentage  
 510 bias of 0.7 % ~ absolute bias of 0.10 mm/day) and Upper Zambezi (0.22 % ~0.23 mm/day),  
 511 PT in the Lower and Middle Zambezi (-0.84 % ~0.18 mm/day) and STB in all the basins (<  
 512 3.70 % ~0.24 mm/day). Gao and Liu (2013) asserts that EZ (a correction process based on  
 513 elevation) is valuable in correcting systematic biases to provide a more accurate precipitation  
 514 input for rainfall-runoff modelling. Significant underestimation for the uncorrected (-21.16 %  
 515 ~0.44 mm/day) and for bias corrected CMORPH are shown for the Upper Zambezi subbasin.  
 516 Note that bias correction effectiveness is similar in the Upper than Lower and Middle Zambezi  
 517 subbasin.

518

519 Figure 6 shows the Taylor diagram for time series of rain gauge (reference) observations vs  
 520 CMORPH bias correction schemes averaged for the Lower Zambezi (UZ), Middle Zambezi  
 521 (MZ) and Upper Zambezi (UZ). The position of each bias correction scheme and uncorrected  
 522 satellite rainfall (R-MORPH) on the plot quantifies how closely the rainfall by R-MORPH  
 523 matches rain gauge observations as well as effectiveness of each of the bias schemes. Overall,  
 524 all bias correction schemes show intermediate performance in terms of bias removal. Only the  
 525 PT and STB for the Lower Zambezi subbasin lie on the line of standard deviation (brown



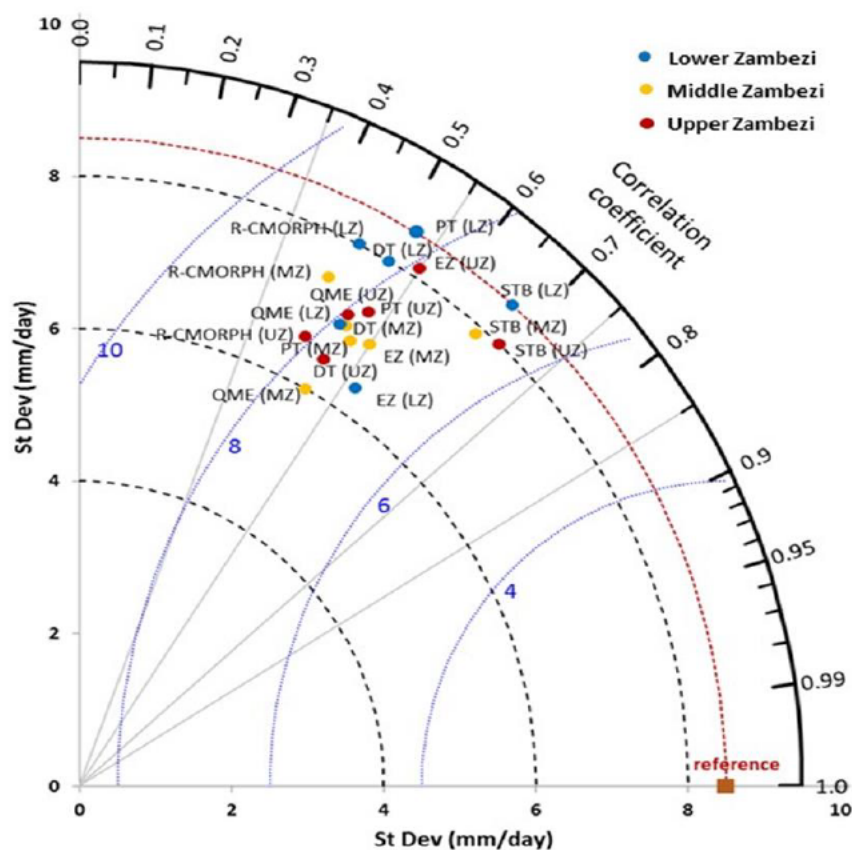


526 dashed arc) and means the standard deviation of the data for the two bias correction schemes  
527 matches the gauge observations. This also indicates that rainfall variations after PT and STB  
528 bias correction for the Lower Zambezi resembles gauge based standard deviation. Note  
529 however that STB performs better than EZ because of superior correlation coefficient.  
530 Compared against the reference line of mean standard deviation (8.5 mm/day), the rainfall  
531 standard deviation for most bias correction schemes is below this line and as such exhibit low  
532 variability across the Zambezi Basin.

533

534 Figure 6 also shows that most of the bias correction schemes have standard deviation range of  
535 6.0 to 8.0 mm/day. There is a consistent pattern between the bias correction schemes that have  
536 low R and high root mean square error difference indicating that these schemes are not effective  
537 in bias removal. Overall, the best performing bias correction schemes (STB and EZ) have  $R >$   
538 0.6, standard deviation relatively close to the reference point and a  $RMSE < 7$  mm/day. The  
539 uncorrected CMORPH (R-MORPH) lies far away from the marked reference (gauge) point on  
540 the x-axis suggesting an intermediate overall effectiveness of the bias correction schemes such  
541 as STB, EZ, DT and PT in removing error as they are relatively closer to the marked reference  
542 point. A shorter distance of all bias correction schemes from the marked reference point would  
543 be preferable. However for much of the Zambezi Basin, the low spatial coverage of rain gauges  
544 imply low spatial dependency of the rain gauges, before a comparison with SREs is done. For  
545 the above reason, studies (e.g. Tian et al., 2010; Lafon et al., 2013) noted that a too sparse gauge  
546 network such as the case in Upper and Middle Zambezi reduces the effectiveness of bias  
547 correction schemes. In the Gilgel Abbay Basin in Ethiopia, increases of R are reported from  
548 0.35 to 0.58 for the STB between 2003-2010 and an improvement of daily root mean square  
549 error from 8 mm/day to 10.5 mm/day (Bhatti et al., 2016). The least performing bias correction  
550 scheme is QME, with a considered low R ( $< 0.49$ ) and standard deviation ( $< 6.5$  mm/day) that  
551 is lower than the reference, but with relatively large RSMD ( $> 8$  mm/day). Inherent to the  
552 methodology of most of bias correction schemes (e.g. QME) is that the spatial pattern of the  
553 SRE does not change and therefore the R for a specific station for daily precipitation does not  
554 necessarily improve. The bias correction results by the Taylor Diagram in Figure 6 corroborates  
555 with findings shown in Figure 4 and Figure 5 for mean, max, ratio of rainfall totals and bias as  
556 performance indicators.

557



558  
 559 Figure 6: Taylor's diagram of statistical comparison between the time series of Rain gauge (reference) observations vs  
 560 CMORPH bias correction schemes averaged for the Lower Zambezi (LZ), Middle Zambezi (MZ), and Upper Zambezi (UZ)  
 561 for the period 1998–2013. The distance of the symbol from point (1, 0) is a relative measure of the bias correction scheme's  
 562 error. The position of each symbol appearing on the plot quantifies how closely that bias correction scheme's precipitation  
 563 pattern matches counterparts by rain gauge. The blue contours indicate the root mean square difference (mm/day)  
 564

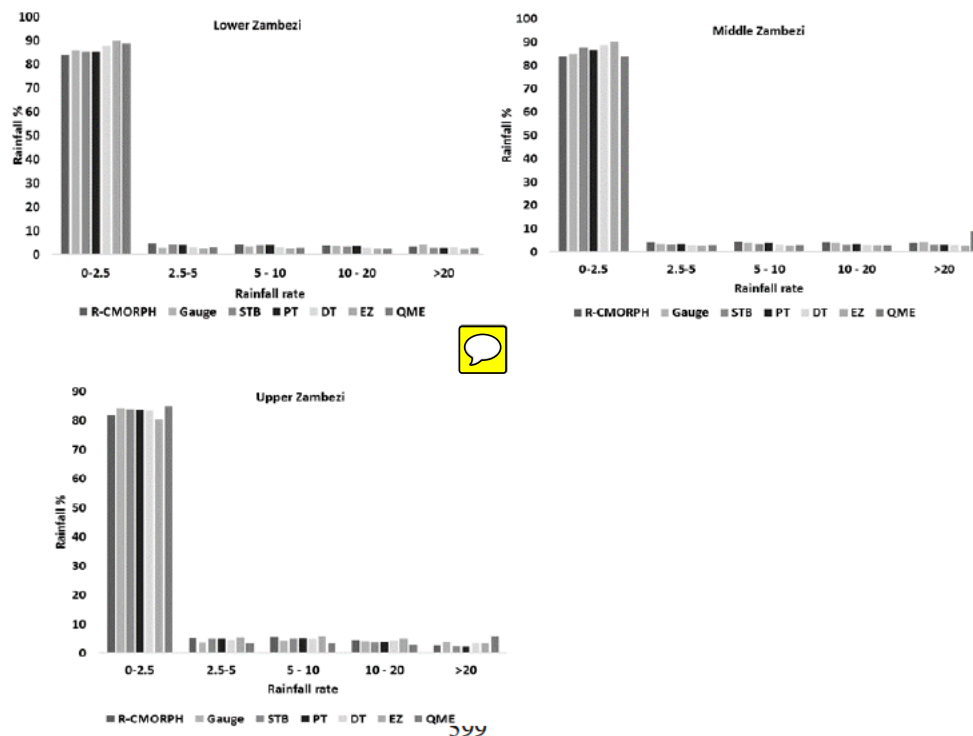
### 565 4.3.2. Classification of CMORPH rainy days

566 The percentage magnitude of rainfall on rainy days in the Zambezi Basin for each bias  
 567 correction scheme is shown in Figure 7. The largest magnitude of rainy days (80–90 %) is  
 568 shown for very light rainfall (0.0–2.5 mm/day). A smaller percentage is shown for 2.5–5.0  
 569 mm/day which is the light rainfall class. Smallest percentage (< 5%) is shown for heavy rainfall  
 570 (> 20.0 mm/day). The CMORPH rainfall corrected with STB, PT and DT matches the gauge  
 571 based magnitude of rainy days in the Lower, Middle and Upper Zambezi suggesting good  
 572 performance. All five bias correction schemes in the Zambezi Basin generally tend to  
 573 overestimate low rainfall magnitudes (< 2.5 mm/day). There is a small difference for moderate  
 574 rainy days classification of 10.0–20.0 mm/day. For QME in the Middle and Upper Zambezi,  
 575 there is overestimation by >80 %. There is underestimation of rainfall for rainy days with  
 576 greater than 20 mm/day. Results are consistent with findings by Gao and Liu (2013) in the  
 577 Tibetan Plateau who also found consistent under and overestimation by CMORPH for rainy



578 days >10.0 mm/day. The study by Zulkafli et al. (2014) in French Guiana and North Brazil  
 579 noted that the low sampling frequency and consequently missed short-duration precipitation  
 580 events between satellite measurements results in underestimation, particularly for heavy  
 581 rainfall.

582 5.



583



600 Figure 7: Percentage of days for rainfall rate classes

601

602 Figure 8 gives the bias correction performance for the different rainy days classes. Results of  
 603 bias removal varies for the Lower, Middle and Upper Zambezi. Comparatively, the STB and  
 604 EZ show effectiveness in bias removal with an average bias correction of 0.97 % and 3.6 % in  
 605 the whole basin respectively. Results show more effectiveness in reducing the percentage bias  
 606 for light rainfall and moderate rainfall (0-2.5 and 5.0-10.0 mmm/day) than the high to very  
 607 high rainfall (10.0-20.0 mm/day and >20.0 mm/day) across the whole basin. The poor  
 608 performance of correction for the heavy rainfall class is caused by, sometimes, large mismatch  
 609 of high rain gauge values versus low CMORPH values. This leads to unrealistically high  
 610 CMORPH values which remain poorly corrected by bias schemes.

611

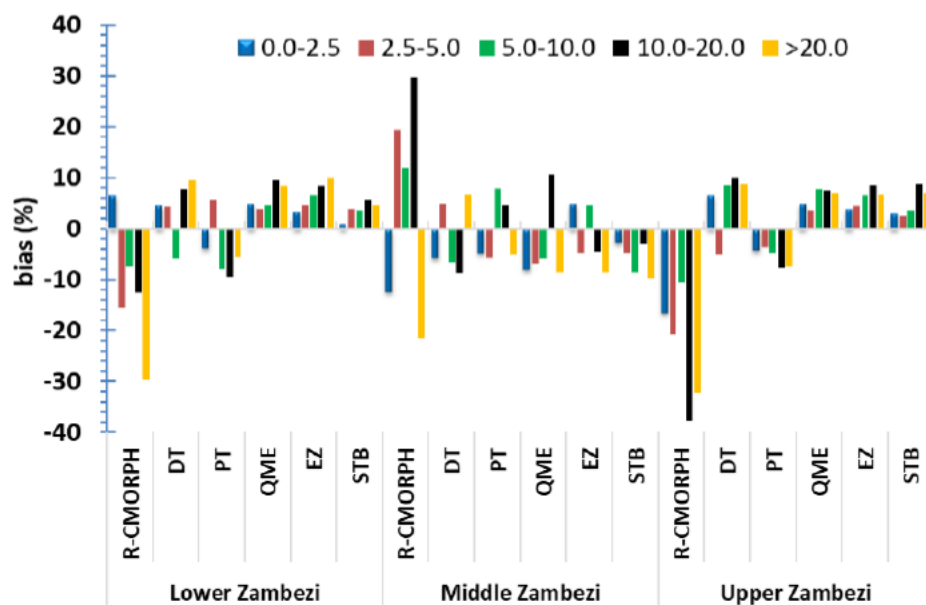


Figure 8: Bias correction (%) for respective rainfall rate classes

612  
 613  
 614  
 615  
 616  
 617  
 618  
 619  
 620  
 621  
 622  
 623  
 624  
 625  
 626  
 627  
 628  
 629  
 630  
 631  
 632  
 633  
 634  
 635  
 636  
 637

### 5.1.1. Seasonal influences on CMORPH bias correction

Table 1 shows bias correction scheme statistics for the dry and wet seasons. Seasonal rainfall here refers to the daily rainfall recorded in specific months belonging to the two defined seasons. Overall, STB, PT and EZ schemes are most effective in correcting errors in CMORPH estimates in the two seasons. The study by Ines and Hansen (2006) for semi-arid eastern Kenya showed that multiplicative bias correction schemes such as STB were effective in correcting the total of the daily rainfall grouped into seasons. Our results show that effectiveness in bias removal in the wet season is higher than in the dry season. Exception is rainfall totals for STB. This is contrary to Vernimmen et al. (2012) who showed that for the dry season, bias for PT decreased in Jakarta, Bogor, Bandung, East Java and Lampung regions after bias correction of monthly TMPA 3B42RT precipitation estimates over the period 2003–2008. Habib (2014) evaluated sensitivity of STB for the dry and wet season and concluded that the bias correction factor for CMORPH shows lower sensitivity for the wet season as compared to the dry season. Our findings also reveal that bias factors for all the schemes are more variable in the dry season than in the wet season and lead to poor performance of the bias correction schemes in the dry season.



638 Table 1: Frequency based statistics for the gauge, uncorrected and bias corrected CMORPH estimates for the dry and wet  
 639 seasons R-Morph is the uncorrected R-CMORPH estimate DT, PT, QME, EZ and STB are the bias corrected rainfall  
 640 estimate Bold values indicate best performance  
 641

Basin	Rainfall Estimate	Dry Season (April-Sept)			Wet Season (Oct-March)		
		Bias (%)	Correlation	Estimated Ratio	Bias (%)	Correlation	Estimated Ratio
Lower Zambezi	R-CMORPH	-49.85	0.39	0.88	-24.1	0.46	0.88
	DT	5.75	0.53	0.82	-6.83	0.59	0.89
	PT	-9.61	0.53	0.87	<b>0.22</b>	0.58	1.02
	QME	8.29	0.52	0.79	-7.34	0.58	0.79
	EZ	8.67	0.54	1.03	-7.61	0.57	1.04
	STB	5.2	0.56	<b>1.02</b>	0.55	0.61	<b>0.99</b>
Middle Zambezi	R-CMORPH	-47.53	0.44	1.11	-18.23	0.39	1.03
	DT	-8.48	0.58	0.92	3.52	0.5	0.94
	PT	-1.63	0.55	1.03	-7.22	0.5	<b>1.01</b>
	QME	-4.33	0.55	0.91	6.07	0.51	0.95
	EZ	-4.48	0.56	1.09	7.4	0.59	1.13
	STB	-3.67	0.56	1.05	2.45	<b>0.62</b>	1.05
Upper Zambezi	R-CMORPH	-58.57	0.4	0.81	-32.13	0.37	0.83
	DT	8.03	0.54	0.75	-8.73	0.49	0.79
	PT	-6.93	0.52	0.82	-5.73	0.5	0.82
	QME	8.12	0.5	0.70	-7.18	0.49	0.7
	EZ	5.17	0.51	0.89	-6.96	<b>0.6</b>	<b>0.99</b>
	STB	<b>2.81</b>	<b>0.59</b>	0.87	-4.9	0.59	0.98

642

643 **6. Conclusions**

644 This study aimed to assess the performance of bias correction schemes for CMORPH rainfall  
 645 estimates in the Zambezi River Basin. The four major conclusions of this study are:

- 646 1. The CMORPH rainfall estimates in the Zambezi Basin are not significantly affected by  
 647 elevation. A similar finding was reported by Gao and Liu (2013) over the Tibetan Plateau  
 648 and Vernimmen et al. (2012) who found a weak relationship between bias errors of SRE  
 649 by influences of elevation. **Our findings contradict findings in** (e.g. Haile et al.,  
 650 2009; Katiraie-Boroujerdy et al., 2013; Rientjes et al., 2013; Wu and Zhai, 2012) who found  
 651 that bias of CMORPH rainfall estimates can be related to elevation ranges. Our study  
 652 further shows that performance of CMORPH is not distinctly related to distance of a large  
 653 water bodies in the Zambezi Basin. **Such** relation was evaluated for rain gauges located  
 654 within specified distances of < 10 km, 10 -50 km, 50 -100 km and > 100 km. **to a large**  
 655 **water body.** Overall findings on bias estimates show that bias of CMORPH estimates is too  
 656 large to allow application of the uncorrected CMORPH product used in this study in  
 657 hydrological and water resources applications in Zambezi Basin.

658



- 659 2. Removing bias (%) in CMORPH is by achieved by STB for Upper, Lower and Middle  
660 subbasins, and by EZ and PT for the Lower and Upper Zambezi. **The STB bias correction**  
661 **scheme effectively adjusted the daily mean of CMORPH estimates by increasing the**  
662 **correlation coefficient by 53% and by reducing the root mean square difference by 25%.**  
663 The EZ and DT were also effective in removing errors related to standard deviation and  
664 ratio of rainfall totals of gauge observations vs CMORPH estimates. Overall, the linear  
665 based correction scheme (STB) that considers space and time variation of SRE bias, is  
666 found more effective in reducing rainfall bias in the basin than the EZ which does not  
667 consider the spatial variability in rainfall. This indicates that the temporal aspect of SRE  
668 bias is more important than the spatial aspect of bias in the Zambezi Basin. In addition, the  
669 multiplicative bias correction schemes (STB and EZ) outperform schemes with power  
670 function correction (PT), quantile mapping (QME) and additive correction (DT). Findings  
671 in this study suggest that a single best bias correction scheme for the entire Zambezi basin  
672 cannot be selected.  
673
- 674 3. We assessed whether bias correction varies for different magnitude of daily rainfall in the  
675 Zambezi Basin. There is overestimation of very light rainfall (< 2.5 mm/day) and  
676 underestimation of very heavy rainfall (>20 mm/day) by the bias correction schemes. Bias  
677 was more effectively reduced for very low to moderate rainfall (< 2.5 and 5.0-10.0  
678 mm/day) than for high to very high rainfall (10.0-20.0 mm/day and >20.0 mm/day).  
679 Overall, the STB and EZ more consistently removed bias in all the rainy days classification  
680 compared to the three other bias correction schemes.  
681
- 682 4. Finally, CMORPH rainfall time series were divided into wet and dry seasonal periods to  
683 assess the influence of seasonality on performance of bias correction schemes. Overall, the  
684 bias correction schemes reveal that bias removal is more effective in the wet season than in  
685 the dry season.  
686

687

#### 688 **Acknowledgements**

689 The study was supported by WaterNet through the DANIDA Transboundary PhD Research in  
690 the Zambezi Basin and the University of Twente's ITC Faculty. The authors acknowledge the  
691 University of Zimbabwe's Civil Engineering Department for platform to carry out this  
692 research.

693

#### 694 **Author Contributions**

695 Webster Gumindoga was responsible for the development of bias correction schemes in the  
696 Zambezi basin. Tom Rientjes was responsible for the research approach and conceptualization.  
697 Tom and Alemseged Haile were responsible for synthesising the methodology and made large  
698 contributions to the manuscript write-up. Hodson Makurira provided some of the rain gauge



699 data and related findings of this study to previous work in the Zambezi Basin. Reggiani Paulo  
700 assisted in interpretation of bias correction results.

701

#### 702 **Conflict of Interests**

703

704 The authors declare no conflict of interests.

705

#### 706 **References**

707 Beilfuss, R., Dutton, P., and Moore, D.: Landcover and Landuse change in the Zambezi Delta,  
708 in: Zambezi Basin Wetlands Volume III Landuse Change and Human impacts, Chapter 2,  
709 Biodiversity Foundation for Africa, Harare, 31-105, 2000.

710 Beilfuss, R.: A Risky Climate for Southern African Hydro: Assessing hydrological risks and  
711 consequences for Zambezi River Basin dams, 2012.

712 Beyer, M., Wallner, M., Bahlmann, L., Thiemig, V., Dietrich, J., and Billib, M.: Rainfall  
713 characteristics and their implications for rain-fed agriculture: a case study in the Upper  
714 Zambezi River Basin, Hydrological Sciences Journal, null-null,  
715 10.1080/02626667.2014.983519, 2014.

716 Bhatti, H., Rientjes, T., Haile, A., Habib, E., and Verhoef, W.: Evaluation of Bias Correction  
717 Method for Satellite-Based Rainfall Data, Sensors, 16, 884, 2016.

718 Bitew, M. M., and Gebremichael, M.: Evaluation of satellite rainfall products through  
719 hydrologic simulation in a fully distributed hydrologic model, Water Resources Research, 47,  
720 2011.

721 Bitew, M. M., Gebremichael, M., Ghebremichael, L. T., and Bayissa, Y. A.: Evaluation of  
722 High-Resolution Satellite Rainfall Products through Streamflow Simulation in a Hydrological  
723 Modeling of a Small Mountainous Watershed in Ethiopia, Journal of Hydrometeorology, 13,  
724 338-350, 10.1175/2011jhm1292.1, 2011.

725 Bouwer, L. M., Aerts, J. C. J. H., Van de Coterlet, G. M., Van de Giessen, N., Gieske, A., and  
726 Manaerts, C.: Evaluating downscaling methods for preparing Global Circulation Model (GCM)  
727 data for hydrological impact modelling. Chapter 2, in Aerts, J.C.J.H. & Droogers, P.

728 (Eds.), Climate Change in Contrasting River Basins: Adaptation Strategies for Water, Food  
729 and Environment. (pp. 25-47). Wallingford, UK: Cabi Press., 2004.

730 Cecinati, F., Rico-Ramirez, M. A., Heuvelink, G. B. M., and Han, D.: Representing radar  
731 rainfall uncertainty with ensembles based on a time-variant geostatistical error modelling  
732 approach, Journal of Hydrology, 548, 391-405,  
733 <http://dx.doi.org/10.1016/j.jhydrol.2017.02.053>, 2017.

734 Cohen Liechti, T., Matos, J. P., Boillat, J. L., and Schleiss, A. J.: Comparison and evaluation  
735 of satellite derived precipitation products for hydrological modeling of the Zambezi River  
736 Basin, Hydrol. Earth Syst. Sci., 16, 489-500, 2012.

737 Cuvelier, C., Thunis, P., Vautard, R., Amann, M., Bessagnet, B., Bedogni, M., Berkowicz, R.,  
738 Brandt, J., Brocheton, F., Bultjes, P., Carnavale, C., Coppalle, A., Denby, B., Douros, J., Graf,  
739 A., Hellmuth, O., Hodzic, A., Honoré, C., Jonson, J., Kerschbaumer, A., de Leeuw, F.,  
740 Minguzzi, E., Moussiopoulos, N., Pertot, C., Peuch, V. H., Pirovano, G., Rouil, L., Sauter, F.,  
741 Schaap, M., Stern, R., Tarrason, L., Vignati, E., Volta, M., White, L., Wind, P., and Zuber, A.:  
742 CityDelta: A model intercomparison study to explore the impact of emission reductions in  
743 European cities in 2010, Atmospheric Environment, 41, 189-207,  
744 <http://dx.doi.org/10.1016/j.atmosenv.2006.07.036>, 2007.



- 745 Dennis, R., Fox, T., Fuentes, M., Gilliland, A., Hanna, S., Hogrefe, C., Irwin, J., Rao, S. T.,  
746 Scheffe, R., Schere, K., Steyn, D., and Venkatram, A.: A framework for evaluating regional-  
747 scale numerical photochemical modeling systems, *Environmental Fluid Mechanics*, 10, 471-  
748 489, [10.1007/s10652-009-9163-2](https://doi.org/10.1007/s10652-009-9163-2), 2010.
- 749 Dinku, T., Chidzambwa, S., Ceccato, P., Connor, S. J., and Ropelewski, C. F.: Validation of  
750 high-resolution satellite rainfall products over complex terrain, *International Journal of Remote*  
751 *Sensing*, 29, 4097-4110, [10.1080/01431160701772526](https://doi.org/10.1080/01431160701772526), 2008.
- 752 Fang, G. H., Yang, J., Chen, Y. N., and Zammit, C.: Comparing bias correction methods in  
753 downscaling meteorological variables for a hydrologic impact study in an arid area in China,  
754 *Hydrol. Earth Syst. Sci.*, 19, 2547-2559, [10.5194/hess-19-2547-2015](https://doi.org/10.5194/hess-19-2547-2015), 2015.
- 755 Fylstra, D., Lasdon, L., Watson, J., and Waren, A.: Design and Use of the Microsoft Excel  
756 Solver, *Interfaces*, 28, 29-55, [doi:10.1287/inte.28.5.29](https://doi.org/10.1287/inte.28.5.29), 1998.
- 757 Gao, Y. C., and Liu, M. F.: Evaluation of high-resolution satellite precipitation products using  
758 rain gauge observations over the Tibetan Plateau, *Hydrol. Earth Syst. Sci.*, 17, 837-849,  
759 [10.5194/hess-17-837-2013](https://doi.org/10.5194/hess-17-837-2013), 2013.
- 760 Gebregiorgis, A. S., Tian, Y., Peters-Lidard, C. D., and Hossain, F.: Tracing hydrologic model  
761 simulation error as a function of satellite rainfall estimation bias components and land use and  
762 land cover conditions, *Water Resources Research*, 48, n/a-n/a, [10.1029/2011wr011643](https://doi.org/10.1029/2011wr011643), 2012.
- 763 Grillakis, M. G., Koutroulis, A. G., Daliakopoulos, I. N., and Tsanis, I. K.: A method to  
764 preserve trends in quantile mapping bias correction of climate modeled temperature, *Earth*  
765 *Syst. Dynam. Discuss.*, 2017, 1-26, [10.5194/esd-2017-53](https://doi.org/10.5194/esd-2017-53), 2017.
- 766 Habib, E., ElSaadani, M., and Haile, A. T.: Climatology-Focused Evaluation of CMORPH and  
767 TMPA Satellite Rainfall Products over the Nile Basin, *Journal of Applied Meteorology and*  
768 *Climatology*, 51, 2105-2121, [10.1175/jamc-d-11-0252.1](https://doi.org/10.1175/jamc-d-11-0252.1), 2012a.
- 769 Habib, E., Haile, A. T., Tian, Y., and Joyce, R. J.: Evaluation of the High-Resolution CMORPH  
770 Satellite Rainfall Product Using Dense Rain Gauge Observations and Radar-Based Estimates,  
771 *Journal of Hydrometeorology*, 13, 1784-1798, [10.1175/jhm-d-12-017.1](https://doi.org/10.1175/jhm-d-12-017.1), 2012b.
- 772 Habib, E., Haile, A., Sazib, N., Zhang, Y., and Rientjes, T.: Effect of Bias Correction of  
773 Satellite-Rainfall Estimates on Runoff Simulations at the Source of the Upper Blue Nile,  
774 *Remote Sensing*, 6, 6688-6708, 2014.
- 775 Haile, A. T., Rientjes, T., Gieske, A., and Gebremichael, M.: Rainfall Variability over  
776 Mountainous and Adjacent Lake Areas: The Case of Lake Tana Basin at the Source of the Blue  
777 Nile River, *Journal of Applied Meteorology and Climatology*, 48, 1696-1717,  
778 [10.1175/2009JAMC2092.1](https://doi.org/10.1175/2009JAMC2092.1), 2009.
- 779 Haile, A. T., Habib, E., and Rientjes, T. H. M.: Evaluation of the climate prediction center CPC  
780 morphing technique CMORPH rainfall product on hourly time scales over the source of the  
781 Blue Nile river, *Hydrological processes*, 27, 1829-1839, 2013.
- 782 Haile, A. T., Yan, F., and Habib, E.: Accuracy of the CMORPH satellite-rainfall product over  
783 Lake Tana Basin in Eastern Africa, *Atmospheric Research*, 163, 177-187,  
784 [http://dx.doi.org/10.1016/j.atmosres.2014.11.011](https://doi.org/10.1016/j.atmosres.2014.11.011), 2015.
- 785 Hempel, S., Frieler, K., Warszawski, L., Schewe, J., and Piontek, F.: A trend-preserving bias  
786 correction - the ISI-MIP approach, *Earth Syst. Dynam.*, 4, 219-236, [10.5194/esd-4-219-2013](https://doi.org/10.5194/esd-4-219-2013),  
787 2013.
- 788 Ines, A. V. M., and Hansen, J. W.: Bias correction of daily GCM rainfall for crop simulation  
789 studies, *Agricultural and Forest Meteorology*, 138, 44-53,  
790 [http://dx.doi.org/10.1016/j.agrformet.2006.03.009](https://doi.org/10.1016/j.agrformet.2006.03.009), 2006.
- 791 Jiang, S.-h., Zhou, M., Ren, L.-l., Cheng, X.-r., and Zhang, P.-j.: Evaluation of latest TMPA  
792 and CMORPH satellite precipitation products over Yellow River Basin, *Water Science and*  
793 *Engineering*, 9, 87-96, [http://dx.doi.org/10.1016/j.wse.2016.06.002](https://doi.org/10.1016/j.wse.2016.06.002), 2016.





- 794 Katiraie-Boroujerdy, P., Nasrollahi, N., Hsu, K., and Sorooshian, S.: Evaluation of satellite-  
795 based precipitation estimation over Iran, Elsevier, Kidlington, ROYAUME-UNI, 15 pp., 2013.
- 796 Khan, S. I., Hong, Y., Gourley, J. J., Khattak, M. U. K., Yong, B., and Vergara, H. J.:  
797 Evaluation of three high-resolution satellite precipitation estimates: Potential for monsoon  
798 monitoring over Pakistan, *Advances in Space Research*, 54, 670-684,  
799 <http://dx.doi.org/10.1016/j.asr.2014.04.017>, 2014.
- 800 Koutsouris, A. J., Chen, D., and Lyon, S. W.: Comparing global precipitation data sets in  
801 eastern Africa: a case study of Kilombero Valley, Tanzania, *Int. J. Climatol.*, 36, 2000-2014,  
802 10.1002/joc.4476, 2016.
- 803 Lafon, T., Dadson, S., Buys, G., and Prudhomme, C.: Bias correction of daily precipitation  
804 simulated by a regional climate model: a comparison of methods, *Int. J. Climatol.*, 33, 1367-  
805 1381, 10.1002/joc.3518, 2013.
- 806 Liu, J., Duan, Z., Jiang, J., and Zhu, A.-X.: Evaluation of Three Satellite Precipitation Products  
807 TRMM 3B42, CMORPH, and PERSIANN over a Subtropical Watershed in China, *Advances*  
808 *in Meteorology*, 2015, 13, 10.1155/2015/151239, 2015.
- 809 Liu, Z.: Comparison of precipitation estimates between Version 7 3-hourly TRMM Multi-  
810 Satellite Precipitation Analysis (TMPA) near-real-time and research products, *Atmospheric*  
811 *Research*, 153, 119-133, <http://dx.doi.org/10.1016/j.atmosres.2014.07.032>, 2015.
- 812 Lo Conti, F., Hsu, K.-L., Noto, L. V., and Sorooshian, S.: Evaluation and comparison of  
813 satellite precipitation estimates with reference to a local area in the Mediterranean Sea,  
814 *Atmospheric Research*, 138, 189-204, <http://dx.doi.org/10.1016/j.atmosres.2013.11.011>, 2014.
- 815 Maraun, D.: Bias Correcting Climate Change Simulations - a Critical Review, *Current Climate*  
816 *Change Reports*, 2, 211-220, 10.1007/s40641-016-0050-x, 2016.
- 817 Marcos, R., Llasat, M. C., Quintana-Seguí, P., and Turco, M.: Use of bias correction techniques  
818 to improve seasonal forecasts for reservoirs — A case-study in northwestern Mediterranean,  
819 *Science of The Total Environment*, 610–611, 64-74,  
820 <https://doi.org/10.1016/j.scitotenv.2017.08.010>, 2018.
- 821 Matos, J. P., Cohen Liechti, T., Juízo, D., Portela, M. M., and Schleiss, A. J.: Can satellite  
822 based pattern-oriented memory improve the interpolation of sparse historical rainfall records?,  
823 *Journal of Hydrology*, 492, 102-116, <http://dx.doi.org/10.1016/j.jhydrol.2013.04.014>, 2013.
- 824 Meyer, H., Dröchner, J., and Nauss, T.: Satellite-based high-resolution mapping of rainfall over  
825 southern Africa, *Atmos. Meas. Tech.*, 10, 2009-2019, 10.5194/amt-10-2009-2017, 2017.
- 826 Moazami, S., Golian, S., Kavianpour, M. R., and Hong, Y.: Comparison of PERSIANN and  
827 V7 TRMM Multi-satellite Precipitation Analysis (TMPA) products with rain gauge data over  
828 Iran, *International Journal of Remote Sensing*, 34, 8156-8171,  
829 10.1080/01431161.2013.833360, 2013.
- 830 Müller, M. F., and Thompson, S. E.: Bias adjustment of satellite rainfall data through stochastic  
831 modeling: Methods development and application to Nepal, *Advances in Water Resources*, 60,  
832 121-134, <http://dx.doi.org/10.1016/j.advwatres.2013.08.004>, 2013.
- 833 Najmaddin, P. M., Whelan, M. J., and Balzter, H.: Application of Satellite-Based Precipitation  
834 Estimates to Rainfall-Runoff Modelling in a Data-Scarce Semi-Arid Catchment, *Climate*, 5,  
835 32, 2017.
- 836 Pereira Filho, A. J., Carbone, R. E., Janowiak, J. E., Arkin, P., Joyce, R., Hallak, R., and Ramos,  
837 C. G. M.: Satellite Rainfall Estimates Over South America – Possible Applicability to the  
838 Water Management of Large Watersheds1, *JAWRA Journal of the American Water Resources*  
839 *Association*, 46, 344-360, 10.1111/j.1752-1688.2009.00406.x, 2010.
- 840 Rientjes, T., Haile, A. T., and Fenta, A. A.: Diurnal rainfall variability over the Upper Blue  
841 Nile Basin: A remote sensing based approach, *International Journal of Applied Earth*  
842 *Observation and Geoinformation*, 21, 311-325, <http://dx.doi.org/10.1016/j.jag.2012.07.009>,  
843 2013.



- 844 Romano, F., Cimini, D., Nilo, S., Di Paola, F., Ricciardelli, E., Ripepi, E., and Viggiano, M.:  
845 The Role of Emissivity in the Detection of Arctic Night Clouds, *Remote Sensing*, 9, 406, 2017.
- 846 Romilly, T. G., and Gebremichael, M.: Evaluation of satellite rainfall estimates over Ethiopian  
847 river basins, *Hydrol. Earth Syst. Sci.*, 15, 1505-1514, 10.5194/hess-15-1505-2011, 2011.
- 848 Seo, D. J., Breidenbach, J. P., and Johnson, E. R.: Real-time estimation of mean field bias in  
849 radar rainfall data, *Journal of Hydrology*, 223, 131-147, [http://dx.doi.org/10.1016/S0022-](http://dx.doi.org/10.1016/S0022-1694(99)00106-7)  
850 [1694\(99\)00106-7](http://dx.doi.org/10.1016/S0022-1694(99)00106-7), 1999.
- 851 Shrestha, M. S.: Bias-adjustment of satellite-based rainfall estimates over the central  
852 Himalayas of Nepal for flood prediction. PhD thesis, Kyoto University, 2011.
- 853 Smiatek, G., Kunstmann, H., and Senatore, A.: EURO-CORDEX regional climate model  
854 analysis for the Greater Alpine Region: Performance and expected future change, *Journal of*  
855 *Geophysical Research: Atmospheres*, 121, 7710-7728, 10.1002/2015JD024727, 2016.
- 856 Srivastava, P. K., Islam, T., Gupta, M., Petropoulos, G., and Dai, Q.: WRF Dynamical  
857 Downscaling and Bias Correction Schemes for NCEP Estimated Hydro-Meteorological  
858 Variables, *Water Resources Management*, 29, 2267-2284, 10.1007/s11269-015-0940-z, 2015.
- 859 Switanek, M. B., Troch, P. A., Castro, C. L., Leuprecht, A., Chang, H. I., Mukherjee, R., and  
860 Demaria, E. M. C.: Scaled distribution mapping: a bias correction method that preserves raw  
861 climate model projected changes, *Hydrol. Earth Syst. Sci.*, 21, 2649-2666, 10.5194/hess-21-  
862 2649-2017, 2017.
- 863 Taylor, K. E.: Summarizing multiple aspects of model performance in a single diagram, *Journal*  
864 *of Geophysical Research: Atmospheres*, 106, 7183-7192, 10.1029/2000JD900719, 2001.
- 865 Tesfagiorgis, K., Mahani, S. E., Krakauer, N. Y., and Khanbilvardi, R.: Bias correction of  
866 satellite rainfall estimates using a radar-gauge product &ndash; a case study in Oklahoma  
867 (USA), *Hydrol. Earth Syst. Sci.*, 15, 2631-2647, 10.5194/hess-15-2631-2011, 2011.
- 868 Themeßl, M. J., Gobiet, A., and Leuprecht, A.: Empirical-statistical downscaling and error  
869 correction of daily precipitation from regional climate models, *Int. J. Climatol.*, 31, 1530-1544,  
870 10.1002/joc.2168, 2010.
- 871 Themeßl, M. J., Gobiet, A., and Heinrich, G.: Empirical-statistical downscaling and error  
872 correction of regional climate models and its impact on the climate change signal, *Clim.*  
873 *Change*, 112, 449-468 2012.
- 874 Thiemig, V., Rojas, R., Zambrano-Bigiarini, M., Levizzani, V., and De Roo, A.: Validation of  
875 Satellite-Based Precipitation Products over Sparsely Gauged African River Basins, *Journal of*  
876 *Hydrometeorology*, 13, 1760-1783, 10.1175/jhm-d-12-032.1, 2012.
- 877 Thiemig, V., Rojas, R., Zambrano-Bigiarini, M., and De Roo, A.: Hydrological evaluation of  
878 satellite-based rainfall estimates over the Volta and Baro-Akobo Basin, *Journal of Hydrology*,  
879 499, 324-338, 10.1016/j.jhydrol.2013.07.012, 2013.
- 880 Thorne, V., Coakley, P., Grimes, D., and Dugdale, G.: Comparison of TAMSAT and CPC  
881 rainfall estimates with raingauges, for southern Africa, *International Journal of Remote*  
882 *Sensing*, 22, 1951-1974, 10.1080/01431160118816, 2001.
- 883 Tian, Y., Peters-Lidard, C. D., and Eylander, J. B.: Real-Time Bias Reduction for Satellite-  
884 Based Precipitation Estimates, *Journal of Hydrometeorology*, 11, 1275-1285,  
885 10.1175/2010JHM1246.1, 2010.
- 886 Toté, C., Patricio, D., Boogaard, H., van der Wijngaart, R., Tarnavsky, E., and Funk, C.:  
887 Evaluation of Satellite Rainfall Estimates for Drought and Flood Monitoring in Mozambique,  
888 *Remote Sensing*, 7, 1758, 2015.
- 889 Tumbare, M. J.: Management of River Basins and Dams: The Zambezi River Basin, edited by:  
890 Tumbare, M. J., Taylor & Francis, 318 pp., 2000.
- 891 Tumbare, M. J.: The Management of the Zambezi River Basin and Kariba Dam, Bookworld  
892 Publishers, Lusaka, 2005.



893 Valdés-Pineda, R., Demaría, E. M. C., Valdés, J. B., Wi, S., and Serrat-Capdevilla, A.: Bias  
894 correction of daily satellite-based rainfall estimates for hydrologic forecasting in the Upper  
895 Zambezi, Africa, *Hydrol. Earth Syst. Sci. Discuss.*, 2016, 1-28, 10.5194/hess-2016-473, 2016.  
896 Vernimmen, R. R. E., Hooijer, A., Mamenun, Aldrian, E., and van Dijk, A. I. J. M.: Evaluation  
897 and bias correction of satellite rainfall data for drought monitoring in Indonesia, *Hydrol. Earth*  
898 *Syst. Sci.*, 16, 133-146, 10.5194/hess-16-133-2012, 2012.  
899 Wehbe, Y., Ghebreyesus, D., Temimi, M., Milewski, A., and Al Mandous, A.: Assessment of  
900 the consistency among global precipitation products over the United Arab Emirates, *Journal of*  
901 *Hydrology: Regional Studies*, 12, 122-135, <http://dx.doi.org/10.1016/j.ejrh.2017.05.002>, 2017.  
902 Woody, J., Lund, R., and Gebremichael, M.: Tuning Extreme NEXRAD and CMORPH  
903 Precipitation Estimates, *Journal of Hydrometeorology*, 15, 1070-1077, 10.1175/jhm-d-13-  
904 0146.1, 2014.  
905 World Bank: The Zambezi River Basin: A Multi-Sector Investment Opportunities Analysis,  
906 Volume 2 Basin Development Scenarios, 2010a.  
907 World Bank: The Zambezi River Basin : A Multi-Sector Investment Opportunities Analysis -  
908 Summary Report. World Bank. © World Bank.  
909 <https://openknowledge.worldbank.org/handle/10986/2958> License: Creative Commons  
910 Attribution CC BY 3.0., 2010b.  
911 Wu, L., and Zhai, P.: Validation of daily precipitation from two high-resolution satellite  
912 precipitation datasets over the Tibetan Plateau and the regions to its east, *Acta Meteorol Sin.*,  
913 26, 735-745, 10.1007/s13351-012-0605-2, 2012.  
914 Yoo, C., Park, C., Yoon, J., and Kim, J.: Interpretation of mean-field bias correction of radar  
915 rain rate using the concept of linear regression, *Hydrological Processes*, 28, 5081-5092,  
916 10.1002/hyp.9972, 2014.  
917 Zulkafli, Z., Buytaert, W., Onof, C., Manz, B., Tarnavsky, E., Lavado, W., and Guyot, J.-L.: A  
918 Comparative Performance Analysis of TRMM 3B42 (TMPA) Versions 6 and 7 for  
919 Hydrological Applications over Andean–Amazon River Basins, *Journal of Hydrometeorology*,  
920 15, 581-592, doi:10.1175/JHM-D-13-094.1, 2014.  
921